THE JOURNAL OF BIOLOGICAL CHEMISTRY VOL. 287, NO. 52, pp. 43685–43693, December 21, 2012

Multivalent Pseudopeptides Targeting Cell Surface Nucleoproteins Inhibit Cancer Cell Invasion through Tissue Inhibitor of Metalloproteinases 3 (TIMP-3) Release*[S]

Received for publication, May 11, 2012, and in revised form, October 4, 2012 Published, JBC Papers in Press, October 29, 2012, DOI 10.1074/jbc.M112.380402

Damien Destouches[‡], Eric Huet[‡], Maha Sader[‡], Sophie Frechault[‡], Gilles Carpentier[‡], Florie Ayoul[‡], Jean-Paul Briand[§], Suzanne Menashi[‡], and José Courty[‡1]

From the [‡]Université Paris-Est, Laboratoire de Recherche sur la Croissance Cellulaire, la Réparation et la Régénération Tissulaires (CRRET), CNRS, 61 avenue du général De Gaulle, 94010 Créteil, France and the [§]CNRS UPR 9021, Institut de Biologie Moléculaire et Cellulaire, Laboratoire d'Immunologie et Chimie Thérapeutique, 15 rue Descartes, 67084 Strasbourg Cedex, France

Background: NucAnt 6L (N6L) binds to nucleoproteins and inhibits tumor growth.
Results: N6L bound to sulfated glycosaminoglycans, induced TIMP-3 release, and inhibited cell invasion. Silencing of TIMP-3 abolished N6L effect on cell invasion.
Conclusion: N6L inhibits cell invasion through the release of TIMP-3.
Significance: TIMP-3 released by N6L inhibits cell invasion. Sulfated glycosaminoglycans are presented as new receptors for N6L.

Blockage of the metastasis process remains a significant clinical challenge, requiring innovative therapeutic approaches. For this purpose, molecules that inhibit matrix metalloproteinases activity or induce the expression of their natural inhibitor, the tissue inhibitor of metalloproteinases (TIMPs), are potentially interesting. In a previous study, we have shown that synthetic ligands binding to cell surface nucleolin/nucleophosmin and known as HB 19 for the lead compound and NucAnt 6L (N6L) for the most potent analog, inhibit both tumor growth and angiogenesis. Furthermore, they prevent metastasis in a RET transgenic mice model which develops melanoma. Here, we investigated the effect of N6L on the invasion capacity of MDA-MB-435 melanoma cells. Our results show that the multivalent pseudopeptide N6L inhibited Matrigel invasion of MDA-MB-435 cells in a modified Boyden chamber model. This was associated with an increase in TIMP-3 in the cell culture medium without a change in TIMP-3 mRNA expression suggesting its release from cell surface and/or extracellular matrix. This may be explained by our demonstrated N6L interaction with sulfated glycosaminoglycans and consequently the controlled bioavailability of glycosaminoglycan-bound TIMP-3. The implication of TIMP-3 in N6L-induced inhibition of cell invasion was evidenced by siRNA silencing experiments showing that the loss of TIMP-3 expression abrogated the effect of N6L. The inhibition of tumor cell invasion by N6L demonstrated in this study, in addition to its previously established inhibitory effect on tumor growth and angiogenesis, suggests that N6L represents a promising anticancer drug candidate warranting further investigation.

In the different processes of tumor progression, including tumor growth, angiogenesis, and invasion, proteolysis of extracellular matrix (ECM)[2] is an essential step (1). Among the enzymes involved in ECM degradation, the most studied is the family of matrix metalloproteinases (MMPs) which contains at least 25 members of metzincin endopeptidases. These enzymes are able to degrade ECM components as well as nonmatrix proteins such as cytokines, chemokines, receptors, antimicrobial peptides, and more (2). MMP activities are well documented in invasive and metastatic cancer, and their increasing expression strongly correlates with poor prognosis in many human malignancies (3–5). Tissue inhibitors of metalloproteinases (TIMPs), which include four members noted TIMP-1 to -4, are natural inhibitors of MMPs. These inhibitors bind to active MMPs in 1:1 molar stoichiometry (6).

Among this family, TIMP-3 has several features that distinguish it from the others TIMPs. TIMPs-1, -2, and -4 are secreted and exist as soluble forms whereas TIMP-3 is tightly associated to ECM through glycosaminoglycan (GAG) binding (7–10). TIMP-3 is able to inhibit all the MMPs (11) and the activity of several adamalysin (ADAM) proteinases including the tumor necrosis factor-converting enzyme (TACE, ADAM-17) (12). Accordingly, TIMP-3 inhibits the shedding of several cell surface proteins such as tumor necrosis factor α (TNFα), and its receptor TNFR1 (13). The antitumor activity of TIMP-3 has been largely demonstrated. Its expression was shown to be silenced by hypermethylation of the gene in malignant tumors such as kidney, colon, breast, brain, and pancreatic cancers (14–17). Accordingly, TIMP-3 overexpression decreased tumor growth in xenograft models including colon carcinoma, melanoma, and neuroblastoma (18–20). TIMP-3 also inhibited angiogenesis, blocking the binding of vascular endothelial

* This work has been funded in part by the Multifunctional Nanotechnology for Selective Detection and Treatment of Cancer (MULTIFUN) program.
[S] This article contains supplemental Experimental Procedures and additional references and Figs. 1–3.
[1] To whom correspondence should be addressed. Tel.: 33-1-45-17-65-24; Fax: 33-1-45-17-18-16; E-mail: courty@u-pec.fr.

[2] The abbreviations used are: ECM, extracellular matrix; A488, Alexa Fluor 488; Btn, biotin; GAG, glycosaminoglycan; MMP, matrix metalloproteinase; N6L, NucAnt 6L; TACE, TNFα-converting enzyme; TIMP, tissue inhibitor of metalloproteinases; TNFR1, TNF receptor 1.

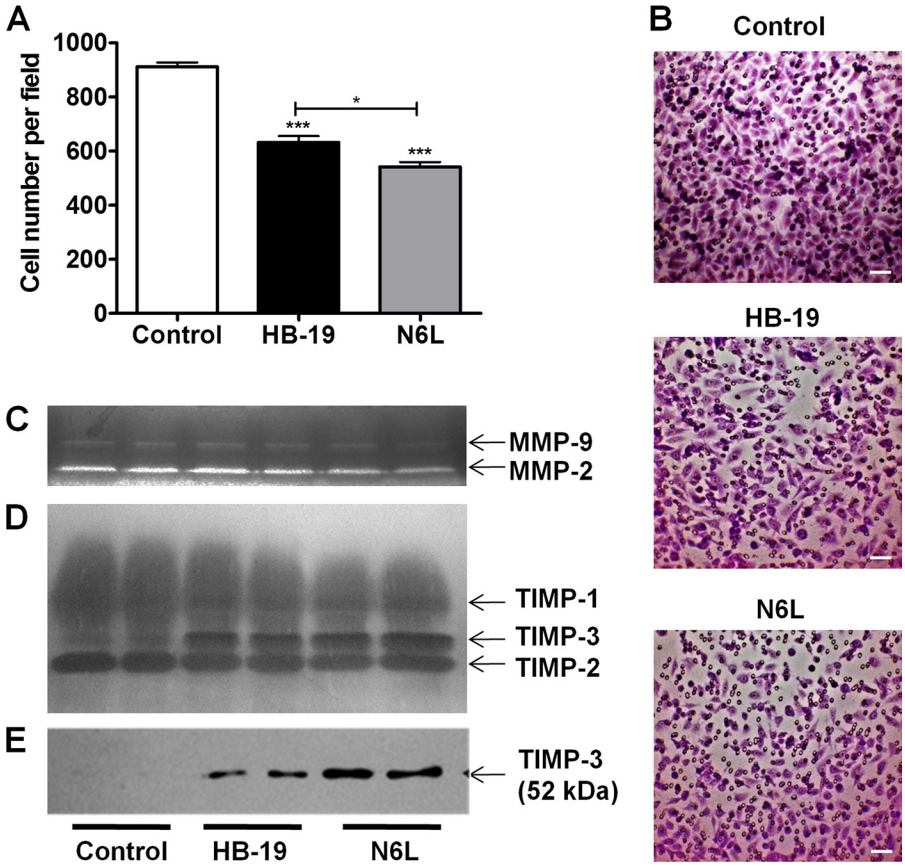

FIGURE 1. **Inhibition of Matrigel invasion induced by N6L and HB-19 treatment is associated with TIMP-3 augmentation in culture media.** *A* and *B*, MDA-MB-435 cells seeded in the upper compartment of modified Boyden chambers containing 20 μg of Matrigel in FBS-free medium and incubated for 24 h for invasion in the presence or not of 10 μM N6L or HB-19. DMEM supplemented with 5% FBS was placed in the lower chamber as chemoattractant. Invading cells were visualized by May-Grünwald/Giemsa staining and counted using ImageJ software (supplemental Fig. 3). *A*, cell number ± S.E. (*error bars*; $n = 4$). *, $p < 0{,}05$; ***, $p < 0{,}001$ statistically significant compared with control. *B*, representative images of membrane after Matrigel invasion by cells. *Scale bars*, 50 μm. *C–E*, MDA-MB-435 cells were treated or not for 48 h at 37 °C with 10 μM N6L or HB-19 in FBS-free medium. Sample loading was normalized using protein concentration of cells lysates. *C*, zymogram for MMP detection in the media conditioned by MDA-MB-435 cells. *D*, reverse zymogram for TIMP detection in the media conditioned by MDA-MB-435 cells. *E*, Western blot analysis for TIMP-3 expression in the media conditioned by MDA-MB-435 cells.

growth factor (VEGF) to its receptor VEGFR2 or blocking angiotensin II receptor activity (21–23).

HB-19 is the prototype of a multivalent pseudopeptides family which was shown to target a nucleoprotein complex at the surface of tumor cells and to induce apoptosis. A more potent HB-19 analog, called NucAnt 6L (N6L), was described more recently. These synthetic peptides were shown to bind two major nucleoproteins, nucleolin and nucleophosmin. Treatment of athymic mice bearing tumor cell xenografts with NucAnt peptides led to tumor growth inhibition by inducing apoptosis of tumor cells and by inhibiting angiogenesis (24, 25). They also delayed tumor development and growth in a spontaneous melanoma model using transgenic RET mice. Furthermore, they decreased the frequency of visceral metastases formation and inhibited melanoma cells adhesion on lungs after injection to the tail vein of mice (26).

In the present study, we demonstrate an inhibitory effect of these multivalent pseudopeptides on human melanoma MDA-MB-435 cells invasion. We present evidence suggesting that the inhibition of invasion observed involves TIMP-3 release from its heparin-sulfate binding sites.

EXPERIMENTAL PROCEDURES

Pseudopeptide Synthesis—HB-19, N6L, and N6L coupled with Alexa Fluor 488 (N6L-A488) or biotin (N6L-Btn) were synthesized as previously described (24, 25).

Cell Culture—Human melanoma MDA-MB-435 cell line was purchased from ATCC (American Type Culture Collection). Cells were routinely cultured in DMEM 4.5 g/liter of glucose (Invitrogen) supplemented with 10% fetal bovine serum (FBS) (Invitrogen) and grown at 37 °C under 5% CO_2 humidified atmosphere.

Matrigel Invasion—MDA-MB-435 invasion assays were performed using 24-well chemotaxis chambers (Transwell, 8 μm, Corning Costar). Transwells were coated with 20 μg of Matrigel™ (BD Biosciences). DMEM supplemented with 5% FBS was placed in the lower chamber as chemoattractant, and 1.5×10^5 cells were seeded in the upper compartment in the presence or not of 10 μM N6L or HB-19. Cells were incubated for 24 h at 37 °C, after which noninvading cells on the upper surface of the filter were removed by wiping with a cotton tip. Cells were then stained with May-Grünwald/Giemsa solution. Pictures of invading cells were taken in three random fields per well (objective ×10). Cell counting was performed by image

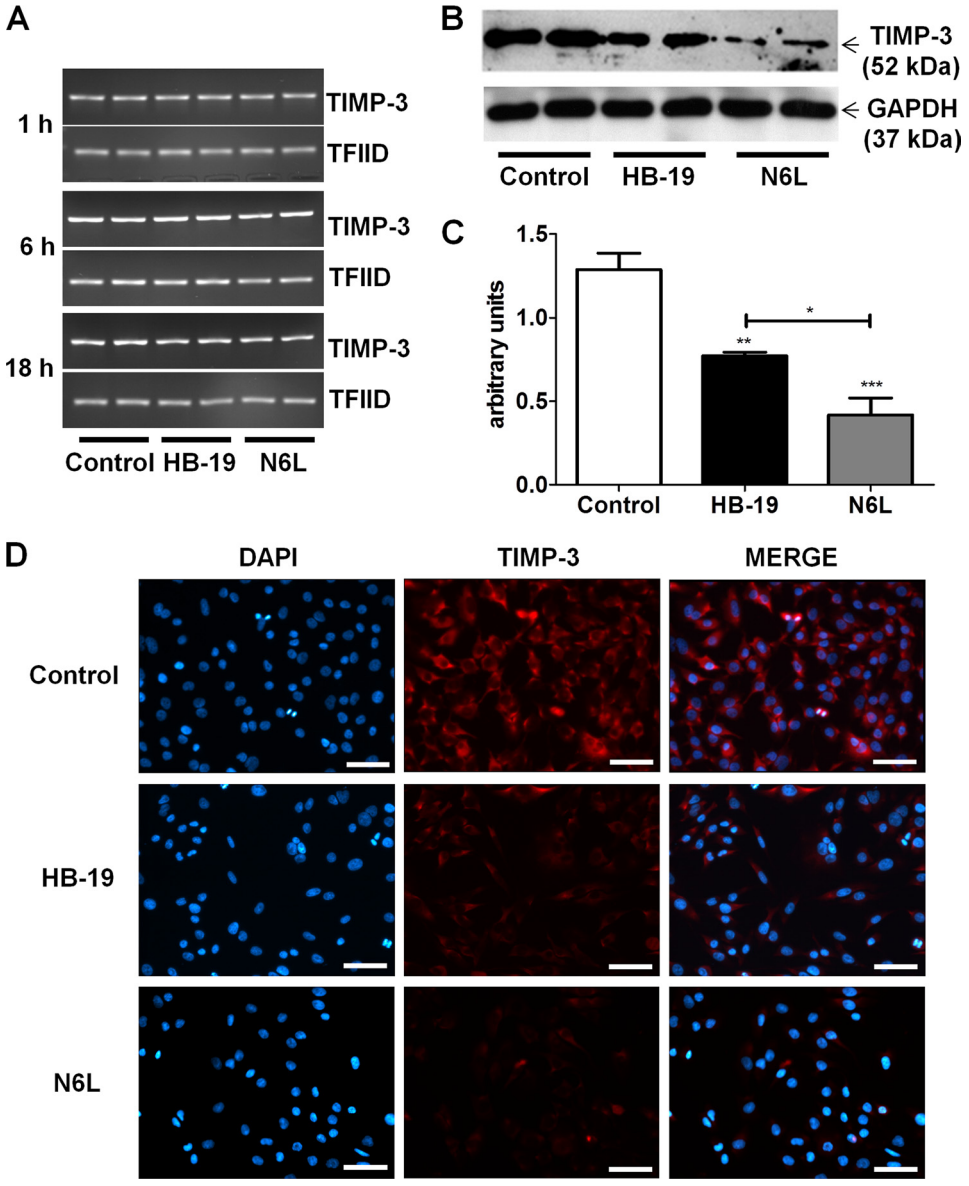

FIGURE 2. **TIMP-3 is released from cell and ECM layer into culture medium.** MDA-MB-435 cells treated for 48 h at 37 °C with or without 10 μM N6L or HB-19 in FBS-free medium. *A*, RT-PCR for TIMP-3 and TFIID mRNA (internal control) was performed at 1, 6, and 18 h after treatment. *B* and *C*, TIMP-3 expression in MDA-MB-435 cell layer analyzed by Western blotting. *B*, representative Western blot. *C*, quantification of TIMP-3 expression from Western blots using measurement of TIMP-3/GAPDH ratio density by ImageJ software *, $p < 0.05$; **, $p < 0.01$; ***, $p < 0.001$ statistically significant. *D*, TIMP-3 immunodetection after 48 h of treatment. MDA-MB-435 cells were washed and fixated with 4% paraformaldehyde, and TIMP-3 was detected using anti-TIMP-3 mouse antibody and analyzed by fluorescent microscopy. Nuclei were stained with DAPI. *Scale bars*, 50 μm.

analysis using an original program, built with the ImageJ software as described in the supplemental Experimental Procedures.

Sample Preparation for Zymography and Western Blot Analysis—MDA-MB-435 cells (2×10^5) were seeded in 12-well plates in DMEM supplemented with 10% FBS and incubated 24 h for adhesion. After two washes with PBS, media were replaced by free FBS DMEM, and cells were treated or not for 48 h at 37 °C with 10 μM N6L or HB-19. Conditioned media were harvested, and cells were lysed in radioimmune precipitation assay buffer (50 mM Tris-HCl, pH 7.5, 150 mM NaCl, 5 mM EDTA, 0.1% SDS, 0.5% Nonidet P-40, 0.5% sodium deoxycholate, 1% protease inhibitor mixture set V (Calbiochem)). Protein concentrations were assessed using the BCA kit (PIERCE) and were used to normalize the samples of conditioned media in the zymography and Western blot analyses (10 μl of culture media loaded corresponding to 2 μg of cell proteins).

Gelatin Zymography and Reverse Zymography—Conditioned media and protein lysates from MDA-MB-435 cells were analyzed for gelatin degradation by electrophoresis under nonreducing conditions on a 10% SDS-polyacrylamide gel containing denatured type I collagen (1 mg/ml). For reverse zymography, active MMP-2 (20 ng/ml) was also added to the polyacrylamide gel as described previously (27).

Western Blotting—Protein samples were separated on a SDS-PAGE under reducing conditions and then transferred onto a 0.45-μm Immobilon-P membrane (Millipore) using standard

protocols. Membranes were blocked with 5% milk, 0.1% Tween 20, TBS, pH 7.4, blocking buffer and incubated with TIMP-3 antibody (mouse monoclonal, clone 136-13H4, Millipore, 1:200), TNFR1 antibody (mouse monoclonal, clone 16805, R&D Systems, 1:250) or GAPDH antibody (mouse monoclonal, clone 6C5, Abcam, 1:100,000) before incubation with secondary anti-mouse antibody (peroxidase-conjugated donkey, Jackson ImmunoResearch Laboratories, 1:10,000). Immunocomplexes were visualized by using the luminescence blotting substrate POD kit (Roche Applied Science) and then by exposure to autoradiography film.

Semiquantitative RT-PCR—MDA-MB-435 cells were seeded and treated in the same conditions as for the zymographic and Western blot analysis. After 1, 6, or 18 h of treatment, cells were washed twice with cold PBS, and RNA was extracted using a TRIzol Reagent kit (Invitrogen), according to the manufacturer's instructions. cDNA was synthesized from 0.5 μg of total RNA using random hexamer primers and the Superscript II™ reverse transcriptase (Invitrogen). 2 μl (1/10) of the reaction products were then submitted to PCR amplification in a final volume of 50 μl. Primers for TIMP-3 detection were: 5′-AGG CAG CAA GCA GAT AGA CT-3′ (forward) and 5′-GCA GGG AGA GGA AAG ACA TT-3′ (reverse) and 5′-AGT GAA GAA CAG TCC AGA CTG-3′ (forward) and 5′-CCA GGA AAT AAC TCG GCT CAT-3′ (reverse) for TFIID detection.

Measure of MMP-2 Activity—Conditioned media (1:20 volume) were mixed with 200 pM recombinant MMP-2 (Calbiochem), in 50 mM Tris, 150 mM NaCl, 5 mM $CaCl_2$, 0.05% Brij35 buffer. 10 μM fluorogenic peptidic substrate Mca-PLGL-Dpa-AR-NH_2 (R&D Systems) was added, and fluorescence was measured using a fluorescence plate reader (Labsystems Fluoroskan II; Thermo Fisher Scientific).

TIMP-3 Immunofluorescence Labeling—MDA-MB-435 cells (5×10^5) were seeded on cover glass in 6-well plates and incubated for 24 h at 37 °C for adhesion. Cells were washed with PBS, treated or not with 10 μM N6L or HB-19 in FBS-free medium for 48 h at 37 °C. Cells were fixed for 10 min with 4% paraformaldehyde at room temperature and saturated with 3% goat serum, PBS for 1 h at room temperature. TIMP-3 was detected using the same antibody used for Western blotting (1:100) and secondary antibody anti-mouse coupled with Alexa Fluor 568 (goat IgG, A11031, Molecular Probes, 1:200). Nuclei were labeled with 1 μg/ml DAPI (Roche Applied Science).

N6L-A488 Cell Labeling—MDA-MB-435 cells seeded as for TIMP-3 labeling were washed with PBS and pretreated or not for 1 h at 37 °C with 0.1 unit/ml heparitinase I, II, III (Sigma), 0.1 units/ml chondroitinase A, B, C (Sigma) in incubation buffer (100 mM Tris-HCl, pH 7.4, 10 mM sodium acetate, 2 mM NaCl). Non-pretreated cells were only incubated with incubation buffer. Cells were labeled with 0.5 μM N6L-A488 for 30 min at 37 °C, washed twice with PBS, and then fixed with methanol for 2 min at room temperature. Nuclei were labeled with 1 μg/ml DAPI (Roche Applied Science).

ELISAs—Heparin (Sigma) was covalently bound to BSA as described previously (28). ELISA plates were coated overnight at 4 °C with heparin-BSA complex (2.5 μg/ml). Wells were saturated 1 h at room temperature with 3% BSA in PBS. Ligands (biotinylated N6L (N6L-Btn) with or not competitors, or recombinant TIMP-3 (Abcam, ab39317) diluted with 1% BSA in PBS, were added to wells and incubated overnight at 4 °C. For competition with TIMP-3 binding, N6L was added for 2 h at 37 °C. N6L-Btn was revealed using anti-biotin antibody coupled to peroxidase (goat antibody, A4541, Sigma, 1:2,000) for 2 h at room temperature. TIMP-3 was revealed using the Millipore antibody for 2 h at 37 °C and secondary anti-mouse antibody (peroxidase-conjugated donkey, Jackson ImmunoResearch Laboratories, 1:10,000) for 1 h at 37 °C. Peroxidase activity was detected using TMB Substrate Kit (Pierce).

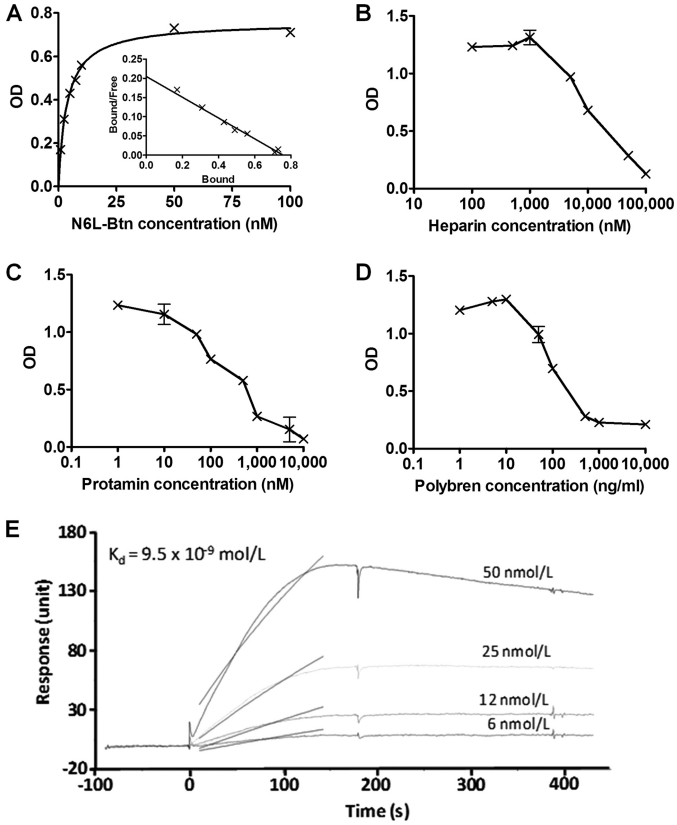

FIGURE 3. **N6L binding to heparin.** *A*, binding of N6L-Btn on heparin. Binding curve and Scatchard analysis (inside) of N6L-Btn on heparin are shown. N6L-Btn was added at different concentrations and incubated overnight at 4 °C on heparin-BSA. N6L-Btn was revealed using anti-biotin antibody coupled to peroxidase. The Scatchard analysis was performed using the GraphPad Prism 4.0 software. *B–D*, binding of 5 nM N6L-Btn on heparin in the presence of different concentrations of heparin (*B*), protamine (*C*), or Polybrene (*D*) as competitor. *E*, direct binding of N6L on heparin used at different concentrations measured in surface plasmon resonance experiment.

Surface Plasmon Resonance—Binding experiments were performed as described previously (25) using biotinylated heparin.

N6L Binding and FACS Analysis—MDA-MB-435 (1×10^5) cells were treated as described for N6L-A488 labeling without methanol fixation and then detached with 2 mM EDTA for 5 min at 37 °C. Fluorescence was analyzed by FACS (MACS Quant, Miltenyi Biotech).

TIMP-3 Silencing by RNA Interference—Validated small interfering sequences of TIMP-3 5′-AGC UGG AGG UCA ACA AGU Att-3′ (Ambion) and 5′-GGC UAC GUC CAG GAG CGC ACC tt-3′ sequence of GFP (MWG) were transfected using Lipofectamine 2000 (Invitrogen) according to the manufacturer's protocols.

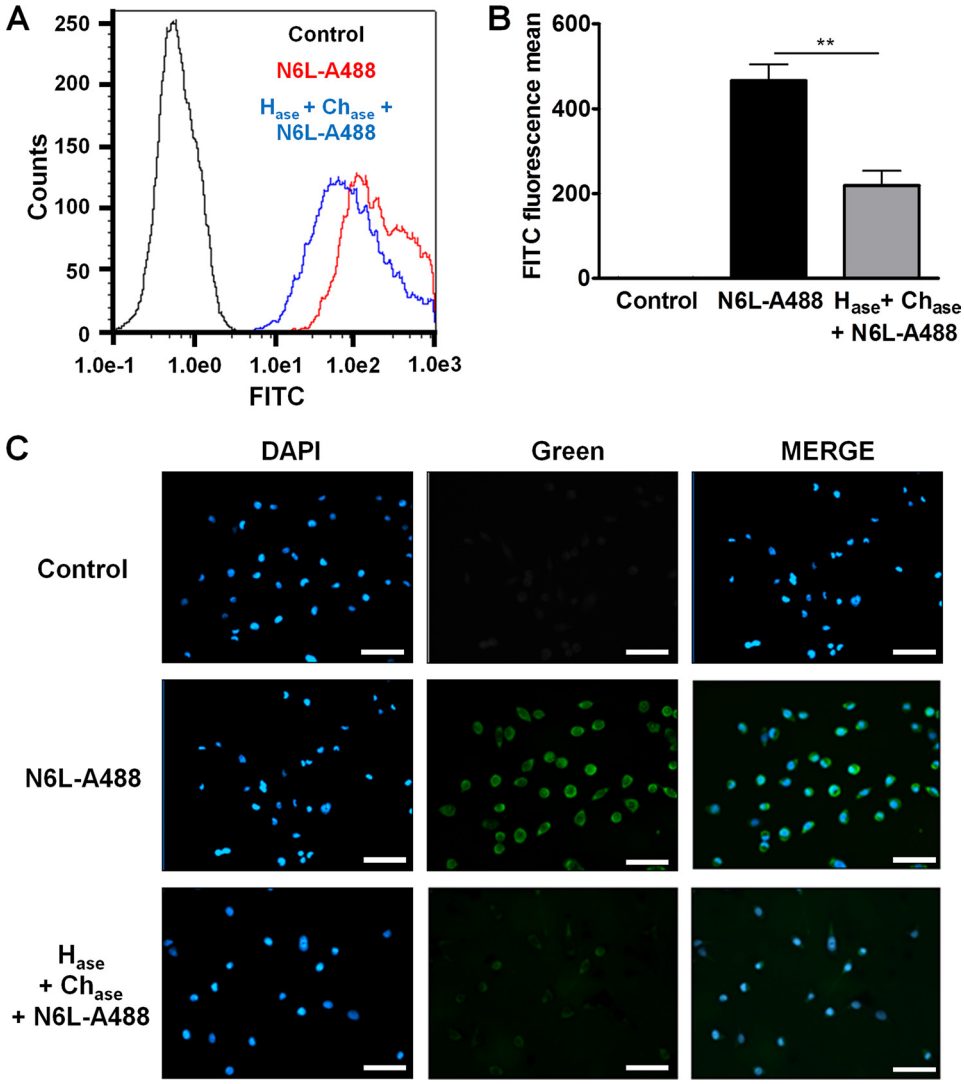

FIGURE 4. **N6L binding to sulfated GAGs on MDA-MB-435 cells.** *A*, fluorescence of nonlabeled MDA-MB-435 cells (*Control*, *black curve*), labeled with 0.5 μM N6L-A488for 30 min at 37 °C (*red curve*) or pretreated with 0.1 unit/ml heparitinase I, II, III (H_{ase}) and 0.1 unit/ml of chondroitinase A, B, C (Ch_{ase}) for 1 h at 37 °C before labeling with 0.5 μM N6L-A488 for 30 min at 37 °C (H_{ase} + Ch_{ase} + N6L-A488, *blue curve*). Fluorescence was analyzed by FACS. *B*, representation of fluorescence means analyzed in *A*. *Error bars*, ± S.E. ($n = 3$). **, $p < 0.01$. *C*, immunofluorescence on nonlabeled MDA-MB-435 cells (*Control*), labeled with 0.5 μM N6L-A488 for 30 min at 37 °C (N6L-A488) or pretreated with 0.1 unit/ml heparitinase I, II, III/chondroitinase A, B, C for 1 h at 37 °C before being labeled with 0.5 μM N6L-A488 for 30 min (H_{ase} + Ch_{ase} + N6L-A488). *Scale bars*, 50 μm.

Statistical Analysis—Statistical significance was determined by ANOVA unpaired *t* test using the Prism 4.0 software (GraphPad, San Diego, CA). Values of $p < 0.05$ were considered significant. Each experiment was performed at least three times.

RESULTS

Inhibition of MDA-MB-435 Cell Invasion by N6L: Implication of MMPs and TIMPs—We first evaluated the effect of N6L on Matrigel invasion by the MDA-MB-435 cells. Cells were seeded in FBS-free media in the upper chambers in the presence or not of either N6L or HB-19 which is another member of the family of multivalent pseudopeptide known to display a lower inhibitory effect than N6L on tumor growth. A N6L concentration of 10 μM was chosen because it does not display activity on MDA-MB-435 cell growth at the conditions used (25) allowing to selectively observe the effect on cell invasion without interference from cell growth effects. FBS 5% was used as chemoattractant in the lower chamber. N6L significantly inhibited cell invasion (39 ± 2.5% inhibition) and that, to a greater extent than with HB-19 (29 ± 3% inhibition) (Fig. 1, *A* and *B*).

The effect of N6L on the expression of MMP-2 and -9 and their natural inhibitors TIMPs was then investigated. For this purpose, cells were treated for 48 h at 37 °C in the presence or not of 10 μM N6L or HB-19. The expression of MMPs and TIMPs in the conditioned media was evaluated respectively by gelatin zymography and reverse gelatin zymography. Inhibition of MMP-2 and -9 was induced by treatment with 10 μM N6L which was not observed with HB-19 used at the same concentration (Fig. 1*C*). Reverse zymography showed that N6L treatment did not cause a noticeable variation of TIMP-2 levels (28 kDa), but caused some inhibition of TIMP-1 (22 kDa). Importantly, a band corresponding to the molecular mass of TIMP-3

(24 kDa) was strongly increased with N6L treatment (Fig. 1*D*). A similar but smaller effect was observed with HB-19. TIMP-3 increase in the culture media after N6L treatment was also observed with human mammary carcinoma MDA-MB 231 cells, human epidermoid carcinoma A431 cells, and murine melanoma B16 cells (data not shown). The increase in TIMP-3 was confirmed by Western blotting using a specific anti-TIMP-3 antibody showing a unique band of 52 kDa which was previously suggested to correspond to TIMP-3 dimers (29, 30) (Fig. 1*E*). These results suggest that TIMP-3 is strongly increased in the culture media after both N6L and HB-19 treatment.

N6L Causes TIMP-3 Release to the Culture Media—To examine whether the increase in TIMP-3 observed in the culture media of N6L- and HB-19-treated cells was due to its increased expression, RT-PCR was performed on the treated cells at 1, 6, and 18 h. However, no variation in TIMP-3 mRNA expression could be observed with time in either the control cells or in treated cells (Fig. 2*A*).

We next analyzed TIMP-3 in the cell lysates by Western blotting to examine the possibility that these pseudopeptides may increase TIMP-3 protein expression by a translational process involving no mRNA modification. Surprisingly, compared with control cells, TIMP-3 was reduced in lysates of treated cells (Fig. 2, *B* and *C*). This was confirmed by immunolabeling analysis of TIMP-3 in MDA-MB-435 cells treated for 48 h with either 10 μM N6L or HB-19, which revealed a decrease in the cell-associated TIMP-3 (Fig. 2*D*). Again, a stronger effect was observed with N6L compared with HB-19. Altogether, these results suggest that TIMP-3 is displaced from the cell surface by the multivalent pseudopeptides and released into culture medium. As N6L displays stronger activity than HB-19, we next focused our studies using N6L exclusively.

TIMP-3 Is Released by N6L through Binding to Heparan Sulfates—We then questioned the mode of action by which N6L can release TIMP-3. We first hypothesized that N6L may have common binding sites as TIMP-3 in the matrix and at the cell surface and can therefore displace TIMP-3 and release it to the extracellular medium. Because TIMP-3 is known to bind to heparan sulfates in the ECM, we examined whether N6L can also bind to heparan sulfates. To this end we used ELISAs to evaluate the binding of biotinylated N6L on heparin-BSA complexes. Our results show that N6L bound to the heparin-BSA in a dose-dependent manner up to a 100 nM concentration (Fig. 3*A*). A 3.7 nM K_d value was calculated by Scatchard analysis, which corresponds to a high affinity binding of N6L to heparin. This high affinity was confirmed by surface plasmon resonance showing a 9.5 nM K_d value (Fig. 3*E*). The absence of heparin or the presence of 100 μM nonbiotinylated N6L as a competitor, used as control conditions, resulted in background levels of binding (supplemental Fig. 1*A*). Protamine and Polybrene, known for their strong interaction with heparin, and free heparin competed with N6L binding with an IC_{50} of 10 μM, 100 ng/ml, and 10 μM, respectively (Fig. 3, *B–D*). Moreover, N6L binding was greatly decreased after treatment of heparin-BSA complex with heparitinases I, II, and III (supplemental Fig. 1*B*). All of these data demonstrate the specificity of the binding of N6L with heparin. In addition, N6L displayed higher affinity to heparin than HB-19, which could explain why N6L displaces more efficiently TIMP-3 than HB-19 (supplemental Fig. 1*C*). To examine whether N6L can also interact with sulfated GAGs present on the cell surface, we analyzed N6L-A488 binding to MDA-MB-435 cells treated or not with heparitinases I, II, and III (H_{ase}) and chondroitinases A, B, and C (Ch_{ase}) which can degrade heparin and chondroitin sulfates, respectively, on the cell surface. Analysis by fluorescence microscopy or FACS revealed that this enzymatic treatment resulted in a significant decrease in cell surface binding of N6L-A488 (Fig. 4). Finally, N6L displaced, in a dose-dependent manner, TIMP-3 binding on heparin in ELISA (Fig. 5*A*). Our results suggest that sulfated GAGs may function as a common receptor for both TIMP-3 and the multivalent pseudopeptides thereby providing a mechanism by which TIMP-3 may be released from the cell surface.

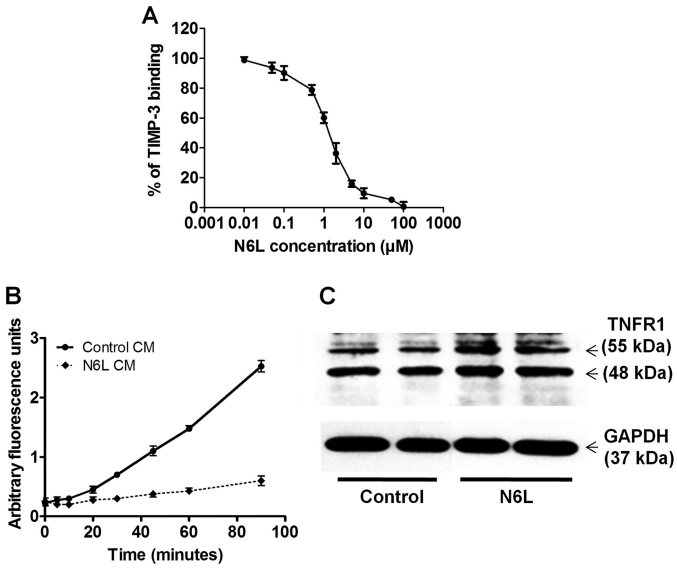

FIGURE 5. **Inhibition of MMP-2 and TACE activity by released TIMP-3.** *A*, dose-dependent displacement of recombinant TIMP-3 (25 nM) binding on heparin by N6L using ELISA test. *B* and *C*, MDA-MB-435 cells were treated or not with 10 μM N6L for 48 h in FBS-free medium. *B*, conditioned media were removed and added to recombinant MMP-2 protein. MMP-2 activity was measured by fluorometry using fluorescent peptidic substrate. *C*, inhibition of TNFR1 cleavage by TACE after N6L treatment. Lysates of nontreated (*Control*) or N6L treated cells were analyzed by Western blotting.

Released TIMP-3 by N6L Retains Its Inhibitory Activities—We next analyzed the effects of the released TIMP-3 on the activity of two of its targets, MMP-2 and TACE. Culture media from cells treated or not with N6L for 48 h were added to recombinant MMP-2. MMP-2 activity was measured using fluorogenic peptidic substrate. Control MMP-2 activity was 0.029 ± 0.002 units/ml, which decreased to 0.005 ± 0.001 units/ml with the N6L-conditioned media corresponding to 84% of inhibition (Fig. 5*A*). No noticeable inhibition could be observed when N6L was added alone to the recombinant MMP-2 demonstrating that N6L did not inhibit MMP-2 activity directly (data not shown).

TIMP-3 is also known as a TACE inhibitor. TNFR1 is a substrate of the TACE that is processed from a 55-kDa membrane form to a 48-kDa soluble form. The effect of TIMP-3 release on TACE activity was evaluated by Western blotting comparing the level of the two TNFR1 forms after treating cells with N6L

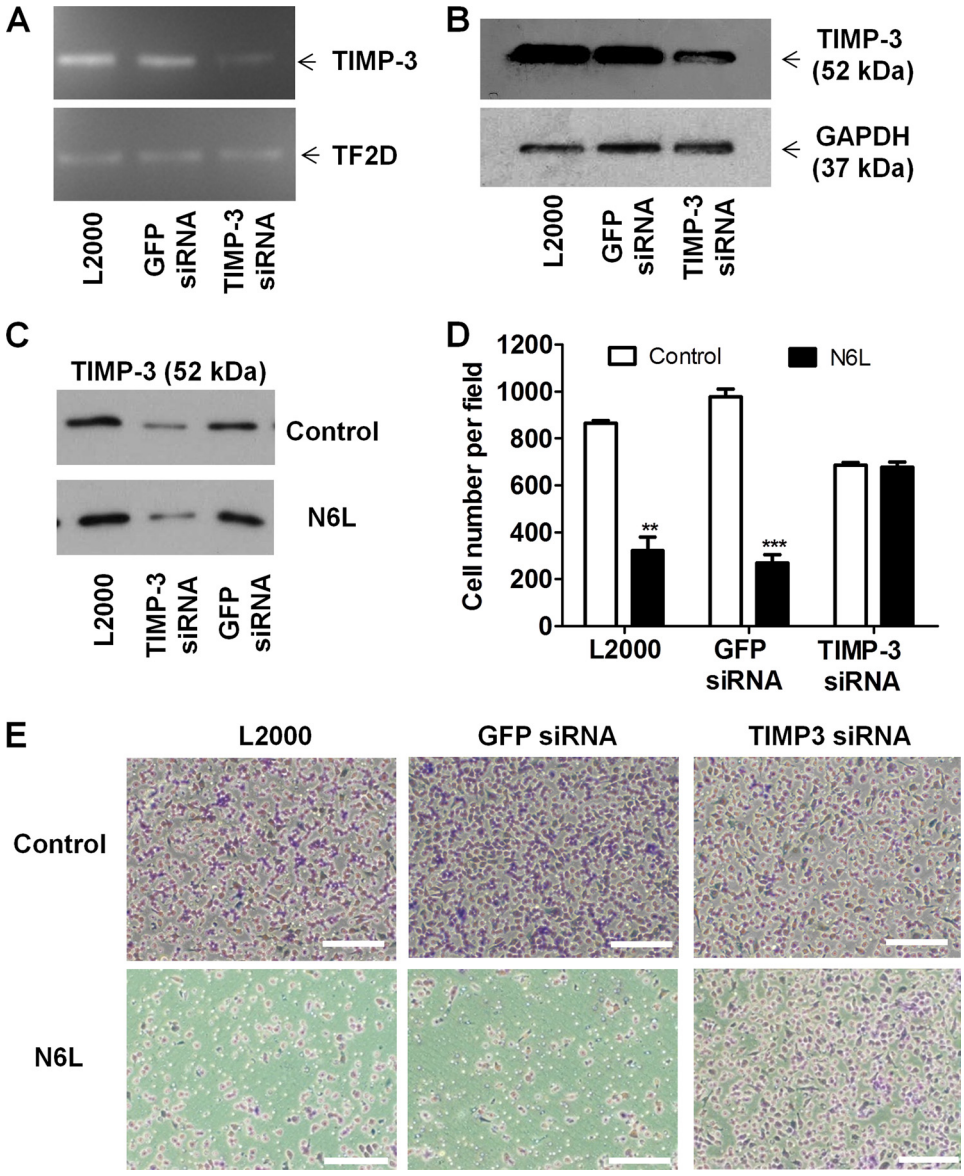

FIGURE 6. **Suppression of N6L inhibitory activity on cell invasion using silencing of TIMP-3 in MDA-MB-435 cells.** MDA-MB-435 cells were transfected for 48 h I 100 nM TIMP-3 siRNA or GFP siRNA as negative control or without siRNA as transfection control (L2000) using Lipofectamine 2000 protocol. *A*, mRNA TIMP-3 expression performed by RT-PCR. *B*, TIMP-3 protein expression analysis performed by Western blotting. *C*, TIMP-3 release from silenced cells or not for TIMP-3 in culture media after 10 μM N6L treatments and analyzed by Western blotting. *D* and *E*, after transfection, cells invasion evaluated in modified Boyden chambers as described in Fig. 1. *D*, cell number $\pm$ S.E. (*error bars*; $n = 4$). **, $p < 0.01$; ***, $p < 0.001$ statistically significant compared with control. *E*, representative pictures of membrane after Matrigel invasion by cells. *Scale bars*, 200 μm.

for 48 h. Such treatment induced an increase in both forms, but the increase was higher in the membrane form of TNFR1 (0.50 of 55-Da form/48-kDa form ratio for control cells compared with 0.77 for N6L) showing TACE inhibition (Fig. 5*B*). These results suggest that TIMP-3 release increases its availability and consequently its activity on MMP-2 and TACE.

N6L Inhibits Cell Invasion through TIMP-3 Release—To determine whether TIMP-3 release may account for the observed inhibition of cell invasion by N6L, TIMP-3 expression was silenced using siRNA transfection.

The inhibition of TIMP-3 expression in cells transfected with TIMP-3 siRNA was confirmed by RT-PCR and Western blotting (Fig. 6*A* and *B*). Lipofectamine 2000 (L2000) and GFP siRNA were used, respectively, as transfection control and negative siRNA control. Transfection with TIMP-3 siRNA abolished N6L-mediated TIMP-3 release to extracellular media (Fig. 6*C*). N6L treatment of TIMP-3 silenced cells no longer inhibited cell invasion (Fig. 6, *D* and *E*). Altogether, these results suggest that the multivalent pseudopeptide N6L inhibits tumor cell invasion by binding to GAGs, thus leading to TIMP-3 release and MMPs activity inhibition.

DISCUSSION

The inhibitory activities of the multivalent pseudopeptides N6L and HB-19 on tumor growth and angiogenesis were demonstrated previously (24, 25). We also identified antimetastatic activity of HB-19 using a RET transgenic mice model which develops spontaneous melanoma, as only 33% of HB-19 treated mice developed visceral metastasis compared with 72% of control mice. In a different model of lung metastasis where mela-

noma T_{III} cells were injected to the tail vein, treatment with HB-19 (at a dose of 5 mg/kg) reduced 43% of cell implantation (26).

The results presented herein show a new mechanism of action of these multivalent pseudopeptides. Both N6L and HB-19 inhibited *in vitro* invasion of human melanoma MDA-MB-435 cells known for their metastatic and invasive properties (31, 32). The inhibitory mechanism was shown to involve release of TIMP-3 from sulfated GAGs present on the cell surface and/or the extracellular matrix, as we demonstrated a high affinity binding of these multivalent pseudopeptides for sulfated GAGs and a displacement of TIMP-3 binding on heparin by ELISA.

The released TIMP-3, shown to retain its activity as it inhibits both MMP-2 and TACE, can then be available to exert its protease inhibitory activity, leading to an inhibition of cell invasion, as observed after HB-19 or N6L treatment. Silencing of TIMP-3 in MDA-MB-435 cells by siRNA transfection abrogated the inhibition of invasion induced by N6L, demonstrating the implication of TIMP-3 in the inhibition of cell invasion induced by N6L. The fact that silencing TIMP-3 in control cells, not treated by N6L, did not increase cell invasion may seem surprising. However, it may underscore the concept that TIMP-3 only exerts its inhibiting effect once released from the cell surface.

TIMP-3 is known to be sequestrated by GAGs contained within the ECM and cell surface. It is thought to interact with heparan sulfates through two sequences rich in lysines and arginines, localized in the A and B β-strands of the N-terminal domain of TIMP-3 (10). It is noteworthy that N6L is rich in lysine and arginine residues which can compete with TIMP-3 for heparan sulfate binding. N6L had no effect on the soluble TIMPs, TIMP-1 and TIMP-2, as their level in the conditioned media of treated cells did not vary significantly. Furthermore, they had no effect on the expression of TIMP-3, as shown by RT-PCR measurement of the mRNAs. Altogether, these results suggest that the multivalent pseudopeptides, by binding to sulfated GAGs, displace TIMP-3 from its heparan sulfate binding sites.

The two previously described targets of N6L and HB-19 were nucleolin and nucleophosmin. These two proteins were first discovered as nucleolus proteins but were later shown to shuttle from the nucleolus to the cell membrane. They are involved in several processes such as ribosome biogenesis, centrosome duplication, apoptosis, and cell proliferation (24, 25, 33, 34). The cell surface N6L targets nucleolin/nucleophosmin were shown to be associated in a nucleoprotein complex also including Wnt-1, gC1q-R, SRP 68/72, as well as several ribosomal proteins (25, 35). It is interesting to note that nucleolin, Wnt-1, and gC1q-R were also described as GAG-binding proteins. Activity of Wnt-1 was shown to be modulated by GAG (36), gC1q-R has been described as a hyaluronan-binding protein (37), and nucleolin was shown to bind the sulfated glycosaminoglycans acharan sulfate leading to inhibition of tumor growth (38). The implication of GAGs in the formation and the activity of this complex remains to be investigated. In addition, the binding of N6L to GAGs concords with the demonstration that N6L can displace the binding of heparin binding growth factors such as VEGF and heparin affin regulatory peptide (HARP, also known as pleiotrophin) from heparin (supplemental Fig. 2). This could explain a previous result showing that HB-19 inhibited angiogenesis induced by HARP or VEGF (24). It also suggests that N6L could block the activity of heparin binding growth factors by avoiding their binding to GAGs and their receptor dimerization leading to growth arrest and cell death.

Furthermore, we have previously demonstrated that N6L induced apoptosis *in vitro* in several cell lines including the human melanoma cells MDA-MB-435 (25). Because TIMP-3 was also shown to induce apoptosis in tumor cells (18, 39, 40), it is tempting to speculate that one of the mechanisms by which N6L induced apoptosis could involve TIMP-3. Indeed, N6L treatment stabilized TNFR1 through the release of TIMP-3. Such an effect was previously reported to increase apoptosis in colon carcinoma and melanoma cells (18, 39).

N6L has shown inhibitory activities on different processes involved in tumor growth such as tumor cell proliferation, angiogenesis, and metastasis. Here, we demonstrated that heparan sulfate is a new additional target of N6L. This effect, added to its binding to nucleolin and nucleophosmin, could explain the pleitrophic actions of N6L. Understanding the mechanisms of action of N6L is essential for its hypothetical pharmaceutical use.

Acknowledgment—We thank M. Decarme (Unité Medyc, Université de Reims Champagne Ardennes, UFR de Médecine, Reims, France) for technical help in MMP activity measurement.

REFERENCES

1. Sahai, E. (2007) Illuminating the metastatic process. *Nat. Rev. Cancer* **7,** 737–749
2. Parks, W. C., Wilson, C. L., and Lopez-Boado, Y. S. (2004) Matrix metalloproteinases as modulators of inflammation and innate immunity. *Nat. Rev. Immunol.* **4,** 617–629
3. Ara, T., Fukuzawa, M., Kusafuka, T., Komoto, Y., Oue, T., Inoue, M., and Okada, A. (1998) Immunohistochemical expression of MMP-2, MMP-9, and TIMP-2 in neuroblastoma: association with tumor progression and clinical outcome. *J. Pediatr. Surg.* **33,** 1272–1278
4. Ribatti, D., Surico, G., Vacca, A., De Leonardis, F., Lastilla, G., Montaldo, P. G., Rigillo, N., and Ponzoni, M. (2001) Angiogenesis extent and expression of matrix metalloproteinase-2 and -9 correlate with progression in human neuroblastoma. *Life Sci.* **68,** 1161–1168
5. Sakakibara, M., Koizumi, S., Saikawa, Y., Wada, H., Ichihara, T., Sato, H., Horita, S., Mugishima, H., Kaneko, Y., and Koike, K. (1999) Membrane-type matrix metalloproteinase-1 expression and activation of gelatinase A as prognostic markers in advanced pediatric neuroblastoma. *Cancer* **85,** 231–239
6. Nagase, H., Visse, R., and Murphy, G. (2006) Structure and function of matrix metalloproteinases and TIMPs. *Cardiovasc. Res.* **69,** 562–573
7. Fariss, R. N., Apte, S. S., Olsen, B. R., Iwata, K., and Milam, A. H. (1997) Tissue inhibitor of metalloproteinases-3 is a component of Bruch's membrane of the eye. *Am. J. Pathol.* **150,** 323–328
8. Leco, K. J., Khokha, R., Pavloff, N., Hawkes, S. P., and Edwards, D. R. (1994) Tissue inhibitor of metalloproteinases-3 (TIMP-3) is an extracellular matrix-associated protein with a distinctive pattern of expression in mouse cells and tissues. *J. Biol. Chem.* **269,** 9352–9360
9. Pavloff, N., Staskus, P. W., Kishnani, N. S., and Hawkes, S. P. (1992) A new inhibitor of metalloproteinases from chicken: ChIMP-3, a third member of the TIMP family. *J. Biol. Chem.* **267,** 17321–17326
10. Yu, W. H., Yu, S., Meng, Q., Brew, K., and Woessner, J. F., Jr. (2000) TIMP-3 binds to sulfated glycosaminoglycans of the extracellular matrix.

J. Biol. Chem. **275,** 31226–31232
11. Brew, K., Dinakarpandian, D., and Nagase, H. (2000) Tissue inhibitors of metalloproteinases: evolution, structure and function. *Biochim. Biophys. Acta* **1477,** 267–283
12. Amour, A., Knight, C. G., Webster, A., Slocombe, P. M., Stephens, P. E., Knäuper, V., Docherty, A. J., and Murphy, G. (2000) The *in vitro* activity of ADAM-10 is inhibited by TIMP-1 and TIMP-3. *FEBS Lett.* **473,** 275–279
13. Edwards, D. R., Handsley, M. M., and Pennington, C. J. (2008) The ADAM metalloproteinases. *Mol. Aspects Med.* **29,** 258–289
14. Bachman, K. E., Herman, J. G., Corn, P. G., Merlo, A., Costello, J. F., Cavenee, W. K., Baylin, S. B., and Graff, J. R. (1999) Methylation-associated silencing of the tissue inhibitor of metalloproteinase-3 gene suggest a suppressor role in kidney, brain, and other human cancers. *Cancer Res.* **59,** 798–802
15. Loging, W. T., and Reisman, D. (1999) Inhibition of the putative tumor suppressor gene TIMP-3 by tumor-derived p53 mutants and wild type p53. *Oncogene* **18,** 7608–7615
16. Pennie, W. D., Hegamyer, G. A., Young, M. R., and Colburn, N. H. (1999) Specific methylation events contribute to the transcriptional repression of the mouse tissue inhibitor of metalloproteinases-3 gene in neoplastic cells. *Cell Growth Differ.* **10,** 279–286
17. Ueki, T., Toyota, M., Sohn, T., Yeo, C. J., Issa, J. P., Hruban, R. H., and Goggins, M. (2000) Hypermethylation of multiple genes in pancreatic adenocarcinoma. *Cancer Res.* **60,** 1835–1839
18. Ahonen, M., Poukkula, M., Baker, A. H., Kashiwagi, M., Nagase, H., Eriksson, J. E., and Kähäri, V. M. (2003) Tissue inhibitor of metalloproteinases-3 induces apoptosis in melanoma cells by stabilization of death receptors. *Oncogene* **22,** 2121–2134
19. Bian, J., Wang, Y., Smith, M. R., Kim, H., Jacobs, C., Jackman, J., Kung, H. F., Colburn, N. H., and Sun, Y. (1996) Suppression of *in vivo* tumor growth and induction of suspension cell death by tissue inhibitor of metalloproteinases (TIMP)-3. *Carcinogenesis* **17,** 1805–1811
20. Mahller, Y. Y., Vaikunth, S. S., Ripberger, M. C., Baird, W. H., Saeki, Y., Cancelas, J. A., Crombleholme, T. M., and Cripe, T. P. (2008) Tissue inhibitor of metalloproteinase-3 via oncolytic herpesvirus inhibits tumor growth and vascular progenitors. *Cancer Res.* **68,** 1170–1179
21. Kang, K. H., Park, S. Y., Rho, S. B., and Lee, J. H. (2008) Tissue inhibitor of metalloproteinases-3 interacts with angiotensin II type 2 receptor and additively inhibits angiogenesis. *Cardiovasc. Res.* **79,** 150–160
22. Ma, D. H., Chen, J. I., Zhang, F., Hwang, D. G., and Chen, J. K. (2003) Inhibition of fibroblast-induced angiogenic phenotype of cultured endothelial cells by the overexpression of tissue inhibitor of metalloproteinase (TIMP)-3. *J. Biomed. Sci.* **10,** 526–534
23. Qi, J. H., Ebrahem, Q., Moore, N., Murphy, G., Claesson-Welsh, L., Bond, M., Baker, A., and Anand-Apte, B. (2003) A novel function for tissue inhibitor of metalloproteinases-3 (TIMP3): inhibition of angiogenesis by blockage of VEGF binding to VEGF receptor-2. *Nat. Med.* **9,** 407–415
24. Destouches, D., El Khoury, D., Hamma-Kourbali, Y., Krust, B., Albanese, P., Katsoris, P., Guichard, G., Briand, J. P., Courty, J., and Hovanessian, A. G. (2008) Suppression of tumor growth and angiogenesis by a specific antagonist of the cell-surface expressed nucleolin. *PLoS One* **3,** e2518
25. Destouches, D., Page, N., Hamma-Kourbali, Y., Machi, V., Chaloin, O., Frechault, S., Birmpas, C., Katsoris, P., Beyrath, J., Albanese, P., Maurer, M., Carpentier, G., Strub, J. M., Van Dorsselaer, A., Muller, S., Bagnard, D., Briand, J. P., and Courty, J. (2011) A simple approach to cancer therapy afforded by multivalent pseudopeptides that target cell-surface nucleoproteins. *Cancer Res.* **71,** 3296–3305
26. El Khoury, D., Destouches, D., Lengagne, R., Krust, B., Hamma-Kourbali, Y., Garcette, M., Niro, S., Kato, M., Briand, J. P., Courty, J., Hovanessian, A. G., and Prévost-Blondel, A. (2010) Targeting surface nucleolin with a multivalent pseudopeptide delays development of spontaneous melanoma in RET transgenic mice. *BMC Cancer* **10,** 325
27. Huet, E., Brassart, B., Cauchard, J. H., Debelle, L., Birembaut, P., Wallach, J., Emonard, H., Polette, M., and Hornebeck, W. (2002) Cumulative influence of elastin peptides and plasminogen on matrix metalloproteinase activation and type I collagen invasion by HT-1080 fibrosarcoma cells. *Clin. Exp. Metastasis* **19,** 107–117
28. Soulié, P., Héroult, M., Bernard, I., Kerros, M. E., Milhiet, P. E., Delbé, J., Barritault, D., Caruelle, D., and Courty, J. (2002) Immunoassay for measuring the heparin-binding growth factors HARP and MK in biological fluids. *J. Immunoassay Immunochem.* **23,** 33–48
29. Hoe, H. S., Cooper, M. J., Burns, M. P., Lewis, P. A., van der Brug, M., Chakraborty, G., Cartagena, C. M., Pak, D. T., Cookson, M. R., and Rebeck, G. W. (2007) The metalloprotease inhibitor TIMP-3 regulates amyloid precursor protein and apolipoprotein E receptor proteolysis. *J. Neurosci.* **27,** 10895–10905
30. Plumb, J., Cross, A. K., Surr, J., Haddock, G., Smith, T., Bunning, R. A., and Woodroofe, M. N. (2005) ADAM-17 and TIMP3 protein and mRNA expression in spinal cord white matter of rats with acute experimental autoimmune encephalomyelitis. *J. Neuroimmunol.* **164,** 1–9
31. Bemis, L. T., and Schedin, P. (2000) Reproductive state of rat mammary gland stroma modulates human breast cancer cell migration and invasion. *Cancer Res.* **60,** 3414–3418
32. Rae, J. M., Creighton, C. J., Meck, J. M., Haddad, B. R., and Johnson, M. D. (2007) MDA-MB-435 cells are derived from M14 melanoma cells: a loss for breast cancer, but a boon for melanoma research. *Breast Cancer Res. Treat.* **104,** 13–19
33. Grisendi, S., Mecucci, C., Falini, B., and Pandolfi, P. P. (2006) Nucleophosmin and cancer. *Nat. Rev. Cancer* **6,** 493–505
34. Srivastava, M., and Pollard, H. B. (1999) Molecular dissection of nucleolin's role in growth and cell proliferation: new insights. *FASEB J.* **13,** 1911–1922
35. Krust, B., El Khoury, D., Nondier, I., Soundaramourty, C., and Hovanessian, A. G. (2011) Targeting surface nucleolin with multivalent HB-19 and related Nucant pseudopeptides results in distinct inhibitory mechanisms depending on the malignant tumor cell type. *BMC Cancer* **11,** 333
36. Reichsman, F., Smith, L., and Cumberledge, S. (1996) Glycosaminoglycans can modulate extracellular localization of the wingless protein and promote signal transduction. *J. Cell Biol.* **135,** 819–827
37. Bourguignon, L. Y. (2008) Hyaluronan-mediated CD44 activation of RhoGTPase signaling and cytoskeleton function promotes tumor progression. *Semin. Cancer Biol.* **18,** 251–259
38. Joo, E. J., ten Dam, G. B., van Kuppevelt, T. H., Toida, T., Linhardt, R. J., and Kim, Y. S. (2005) Nucleolin: acharan sulfate-binding protein on the surface of cancer cells. *Glycobiology* **15,** 1–9
39. Smith, M. R., Kung, H., Durum, S. K., Colburn, N. H., and Sun, Y. (1997) TIMP-3 induces cell death by stabilizing TNF-α receptors on the surface of human colon carcinoma cells. *Cytokine* **9,** 770–780
40. Deng, X., Bhagat, S., Dong, Z., Mullins, C., Chinni, S. R., and Cher, M. (2006) Tissue inhibitor of metalloproteinase-3 induces apoptosis in prostate cancer cells and confers increased sensitivity to paclitaxel. *Eur. J. Cancer* **42,** 3267–3273